Japanese Journal of Radiology (2019) 37:81–87
https://doi.org/10.1007/s11604-018-0785-5

ORIGINAL ARTICLE

The feasibility of dedicated breast PET for the assessment of residual tumor after neoadjuvant chemotherapy

Hiromi Koyasu[1,2] · Satoshi Goshima[1] · Yoshifumi Noda[1] · Hironori Nishibori[2] · Makoto Takeuchi[3] · Kengo Matsunaga[4] · Tetsuya Yamada[4] · Masayuki Matsuo[1]

Received: 15 August 2018 / Accepted: 9 October 2018 / Published online: 3 November 2018

Abstract

Purpose To evaluate the utility of ring-type dedicated breast positron emission tomography (dbPET) for the detection of the residual tumor after neoadjuvant chemotherapy (NAC).

Materials and methods This prospective study included 27 women with histologically proven breast cancer over a 37-month period. All patients underwent ring-type dbPET followed by whole-body PET-CT (WBPET) for preoperative tumor evaluation and re-staging after NAC. The maximum standardized uptake value (SUV_{max}) of the tumor lesion and the degree of confidence for the presence of the residual tumor were compared between pathological complete response (pCR) and non-pCR tumors. The sensitivity, specificity, and area under the receiver operating characteristic curve (AUC) for the detection of a non-pCR tumor were compared between dbPET and WBPET.

Results On dbPET, SUV_{max} was significantly higher in non-pCR than in pCR tumors ($P=0.030$). The sensitivity for the detection of a non-pCR tumor was significantly higher with dbPET than with WBPET (84.2% vs 26.3%, $P=0.001$). In the qualitative analysis, the sensitivity for the detection of a non-pCR tumor was also significantly higher with dbPET than with WBPET (57.9% vs 21.1%, $P=0.016$).

Conclusion The dbPET can provide more sensitive detection of residual tumor after NAC than can WBPET.

Keywords Breast cancer · Dedicated breast positron emission tomography · Whole-body PET-CT · Residual tumor · Neoadjuvant chemotherapy

✉ Satoshi Goshima
gossy@par.odn.ne.jp

Hiromi Koyasu
hiromi11_br@yahoo.co.jp

Yoshifumi Noda
noda1031@gifu-u.ac.jp

Hironori Nishibori
verybori@gmail.com

Makoto Takeuchi
m-takeuchi@kizawa-memorial-hospital.jp

Kengo Matsunaga
matsunaga-path@umin.net

Tetsuya Yamada
tty-yama@kizawa-memorial-hospital.jp

Masayuki Matsuo
masa-uw@hotmail.co.jp

1 Department of Radiology, Gifu University, 1-1 Yanagido, Gifu 501-1194, Japan

2 Department of Radiology, Kizawa Memorial Hospital, Minokamo, Japan

3 Department of Breast Surgery, Kizawa Memorial Hospital, Minokamo, Japan

4 Department of Pathology, Kizawa Memorial Hospital, Minokamo, Japan

Introduction

Positron emission tomography (PET) with fluorine 18 fluorodeoxyglucose (^{18}F-FDG) is an essential imaging modality for diagnosing breast cancer, especially in the staging or diagnosis of recurrence [1]. Most breast cancers overexpress glucose transporters 1 and 3, as well as showing increased hexokinase activity [2, 3]. However, FDG-PET imaging has some limitations regarding the assessment of primary lesions, including poor sensitivity for assessing small tumors, particularly those with a maximum diameter < 10 mm [4]. This is because the spatial resolution of PET is limited and, in some cases, the uptake of FDG by a tumor is affected by characteristics such as a low nuclear grade, ductal carcinoma in situ, and lobular carcinoma [4, 5]. FDG-PET has, therefore, mainly been used for detecting lymph node and/or distant metastases, rather than for locoregional tumor assessment. To overcome these limitations, dedicated breast PET (dbPET) has been under development since 1994 [6]. This imaging modality improves the detectability of small and/or low-contrast lesions through its high spatial resolution and good energy resolution [7, 8].

Recently, neoadjuvant chemotherapy (NAC) has become standard therapy for locally advanced breast cancer. NAC has several advantages, including downsizing the primary tumor to enable breast-conserving surgery [9] and allowing a preoperative assessment of the effectiveness of systemic chemotherapy for the tumor. In addition, several studies have demonstrated that pathological complete response (pCR) after NAC is predictive of improved disease-free and overall survival [10–12]. A preoperative assessment of the presence or absence of residual tumor is crucial for the patient's prognosis.

Morphological tumor assessments using mammography or ultrasonography are widely used for evaluating the response to NAC. However, these modalities tend to overestimate the tumor volume because chemotherapy induces tumor necrosis and fibrosis [13]. Recently, magnetic resonance imaging (MRI) has been recommended for evaluating the response to NAC [13]. However, it can be difficult with MRI to distinguish viable tumor tissue from fibrotic scar tissue and to depict scattered lesions [14]. We hypothesized that dbPET may provide better visualization of the metabolic activity of very small residual tumors. The purpose of this study was to evaluate the feasibility of dbPET for the assessment of residual tumor after NAC.

Materials and methods

Patient

This prospective study was approved by our institutional review board, and written informed consent was obtained from all the patients. Between April 2015 and April 2018, 27 patients (mean age 55.4 ± 7.9 years; range 42–67 years) with breast cancer underwent both conventional whole-body PET-CT (WBPET) and ring-type dbPET for preoperative tumor assessment and re-staging after NAC at our institution. None experienced any unexpected events; so, all 27 were included in this study. All the lesions were preoperatively diagnosed by core needle biopsy as invasive ductal carcinoma, and all were surgically resected after the NAC. The mean interval between PET examination and surgical resection was 17.2 days (range 6–31 days).

NAC regimen

The patients received one–four cycles of anthracycline followed by four cycles of taxane regimen. In addition, 11 of the patients with human epidermal growth factor receptor 2 (HER2)-positive disease received four cycles of trastuzumab, and one of these patients additionally received four cycles of bevacizumab. Two patients could not complete the regimens because of side effects.

Scanning protocols

WBPET was performed with an Eminence SOPHIA PET scanner (Shimadzu, Kyoto, Japan) and dbPET with an Elmammo system (Shimadzu, Kyoto, Japan). The scan parameters are summarized in Table 1. The patient was instructed to fast for at least 6 h prior to the scan. ^{18}F-FDG was injected intravenously at a dose of 0.1 mCi (3.7 MBq)/kg body weight, and 45 min later, the WBPET was acquired in the mid-expiration phase of free breathing, with continuous bed motion at a speed of 1.0 mm/s. The scan included an area from the vertex to mid-thigh with the images acquired continuously. The transmission scan was performed using a cesium-137 point source, with the emission scan performed simultaneously. The CT parameters were as follows: table feed per rotation, 1.4 mm; rotation time, 0.75 s; tube voltage, 120 kVp; quality reference, 97.5 mAs; and field of view, 59 cm. Once the WBPET image acquisition was complete, dbPET was performed with the patient in a prone position with her breast hanging down into the ring-type detector. The scan was acquired unilaterally from right to left. Each scan took 7 min.

Histological assessment of therapeutic response

Each patient's therapeutic response to NAC was evaluated histopathologically by two pathologists (T.Y. and K.M., with 21 and 33 years of experience in oncologic pathology, respectively). They classified the response according to the Japan Breast Cancer Society criteria [15], as follows: grade 0, no response; grade 1, slight response (1a, mild response;

Table 1 The specification of the equipment and collection conditions

	WBPET	DbPET
	Eminence-Sophia (Shimadzu, Kyoto, Japan)	Elmammo (Shimadzu, Kyoto, Japan)
Detector	BGO	LGSO
Detector size (mm)	3.5 × 6.25 × 30	1.44 × 1.44 × 18
Axial FOV/opening width (mm)	208/600	155/185
Collection mechanism	3D	3D
FWHM (mm)	4.5	≤ 1.5
Transmission scan (min)	16–20 (continuous)	–
Emission scan (min)	16–20 (continuous)	7 (static)
Reconstruction	3D-DRAMA	List-DRAMA
Scatter correction	Deconvolution	Deconvolution
Iteration	1	1
Subset (filter cycle)	128	128
Collection matrix	128 × 128	236 × 236

WBPET whole-body positron emission tomography, *dbPET* dedicated breast positron emission tomography, *FOV* field of view, FWHM full width at half maximum, *BGO* bismuth germinate: $Bi_4Ge_3O_{12}$, *LGSO* lutetium gadolinium oxyorthosilicate: $Lu_{2\text{-}X}Gd_XSiO_5$:Ce, *DRAMA* dynamic row-action maximum likelihood algorithm

1b, moderate response); grade 2, marked response (2a, high response; 2b, extremely high response); and grade 3, complete response. According to these criteria, a pathological complete response (pCR) is one where the invasive tumor has disappeared, regardless of the presence or absence of a ductal component.

Quantitative image analysis

A radiologist (H.M., with 12 years of experience in the interpretation of PET images) placed a region of interest (ROI) that encompassed the entire tumor on the WBPET and dbPET axial images using a commercially available Digital Imaging and Communications in Medicine viewer, and measured the maximum standardized uptake value (SUV_{max}) for each modality. If there was no noticeable tumor FDG uptake on the images acquired after NAC, the radiologist placed the ROI where the tumor had been present on the pretreatment images.

Qualitative image analysis

Two radiologists (Y.N. and H.K., with 7 and 10 years of experience in the interpretation of PET images, respectively) interpreted the WBPET and dbPET images in a random order and evaluated the degree of confidence for the presence of residual tumor using a five-point scale: (1) no uptake (residual tumor is highly unlikely to be present); (2) slight uptake (residual tumor is unlikely to be present); (3) moderate uptake (the presence of residual tumor is equivocal); (4) high uptake (residual tumor is likely to be present); and (5) marked uptake (residual tumor is highly likely to be present). The evaluation was made by consensus between the two radiologists.

Statistical analysis

We compared the patients' characteristics between pCR and non-pCR tumors using Mann–Whitney *U* and Fisher's tests. For the quantitative image analysis, the Mann–Whitney *U* test was conducted to evaluate differences in SUV_{max} between pCR and non-pCR tumors. Receiver operating characteristic (ROC) curves were used to calculate the sensitivity, specificity, and area under the ROC curve (AUC) for each modality for the detection of a non-pCR tumor. An optimal cutoff value that yielded the maximal sensitivity and specificity for the detection of a non-pCR tumor was determined from the ROC curve. The AUCs for the detection of non-pCR tumor were compared between WBPET and dbPET using the method of Hanley and McNeil. For the qualitative image analysis, the Mann–Whitney *U*, McNemar, and Fisher's tests were used to compare the confidence ratings, sensitivity, specificity, positive predictive value (PPV), and negative predictive value (NPV) for the detection of a non-pCR tumor between WBPET and dbPET. The sensitivity for the detection of a non-pCR tumor was determined from the number of patients assigned grade 3, 4, or 5 as a proportion of the total number of patients with a non-pCR tumor. Similarly, the specificity was determined from the number of patients assigned grade 1 or 2 as a proportion of the total number of patients without a non-pCR tumor. The statistical analyses were performed using MedCalc

Software, version 18.5. A P value < 0.05 was considered to be significant.

Results

Patient background factors and tumor characteristics

Table 2 summarizes the patient and tumor characteristics. There was no significant difference between the patients with pCR and non-pCR tumors in age ($P = 0.084$) or the proportions of histopathological subtypes ($P = 0.53$). However, there were significant differences in the proportion of each grade of therapeutic response to NAC ($P < 0.001$) and the size of residual tumor ($P = 0.013$).

Quantitative image analysis

The measurements of SUV_{max} are summarized in Table 3. The SUV_{max} was significantly higher on dbPET than on WBPET ($P \leq 0.003$). On dbPET, the SUV_{max} was significantly higher in non-pCR tumors than in pCR tumors (3.90 ± 3.15 vs 2.28 ± 0.60, $P = 0.030$); whereas, there was no significant difference on WBPET (1.60 ± 0.92 vs 1.22 ± 0.30, $P = 0.30$) (Fig. 1). The ROC optimal cutoff values for detecting a non-pCR tumor on WBPET and dbPET were 1.77 and 2.2, respectively. Using these cutoff values, the sensitivity, specificity, and AUC for the detection of a non-pCR tumor on WBPET were 26.3%, 100%, and 0.63, respectively, and on dbPET were 84.2%, 62.5%, and 0.77. There was a statistically significant difference between WBPET and dbPET in sensitivity ($P = 0.0010$), but not in specificity ($P = 0.25$) or AUC ($P = 0.34$).

Qualitative image analysis

The qualitative results are summarized in Table 4. For non-pCR tumors, the confidence rating for the presence of residual tumor was significantly higher on dbPET than on WBPET (3.1 ± 1.9 vs 1.5 ± 1.3, $P = 0.007$), but there was no significant difference in pCR tumors (1.0 ± 0.0 vs 1.8 ± 1.4, $P = 0.10$). The sensitivity for the detection of residual tumor was significantly higher on dbPET than on WBPET (57.9% vs 21.1%, $P = 0.016$) (Table 4 and Fig. 2). There were no significant differences between WBPET and dbPET in specificity, PPV, NPV, or AUC ($P = 0.49–1.00$).

Table 2 Patient background factors and tumor characteristics

Characteristics	pCR	Non-pCR	*P* value
Number of patients	8	19	NA
Age, year	59.0 ± 5.0 (53–66)	53.1 ± 8.6 (42–67)	0.084
Subtype			
Luminal A	0 (0%)	6 (31.6%)	0.53
Luminal B	6 (75.0%)	6 (31.6%)	
HER2 enriched	0 (0%)	2 (10.5%)	
Triple negative	2 (25.0%)	5 (26.3%)	
Therapeutic response			
G0	0 (0.0%)	5 (26.3%)	< 0.001*
G1a	0 (0.0%)	1 (5.3%)	
G1b	0 (0.0%)	3 (15.8%)	
G2a	0 (0.0%)	4 (21.1%)	
G2b	0 (0.0%)	6 (31.6%)	
G3 with ductal component	5 (62.5%)	0 (0.0%)	
G3 without ductal component	3 (37.5%)	0 (0.0%)	
Size of residual tumor			
0 mm	3 (37.5%)	0 (0.0%)	0.013*
< 5 mm	5 (62.5%)	10 (52.6%)	
5 mm ≥ , < 10 mm	0 (0.0%)	6 (31.6%)	
10 mm ≥ , < 15 mm	0 (0.0%)	1 (5.3%)	
15 mm ≥ , < 20 mm	0 (0.0%)	2 (10.5%)	
20 mm ≥	0 (0.0%)	0 (0.0%)	

HER human epidermal growth factor receptor, *pCR* pathological complete response, *NA* not applicable

*$P < 0.05$, significant difference

Table 3 Quantitative diagnostic performance for the detection of non-pCR tumor between WBPET and dbPET

	WBPET	DbPET	*P* value
SUV_{max}			
pCR	1.22 ± 0.30	2.28 ± 0.60	< 0.001*
Non-pCR	1.60 ± 0.92	3.90 ± 3.15	0.003*
P value	0.30	0.030*	NA
Diagnostic performance			
Cutoff value	1.77	2.2	NA
Sensitivity	26.3%	84.2%	0.0010*
Specificity	100%	62.5%	0.25
AUC (95% CI)	0.63 (0.42–0.81)	0.77 (0.57–0.91)	0.34

Data are means ± 1 standard deviation with ranges in parentheses

WBPET whole-body positron emission tomography, *dbPET* dedicated breast positron emission tomography, SUV_{max} the maximum standardized uptake value, *pCR* pathological complete response, *CI* confidence interval, *NA* not applicable

*$P < 0.05$, significant difference

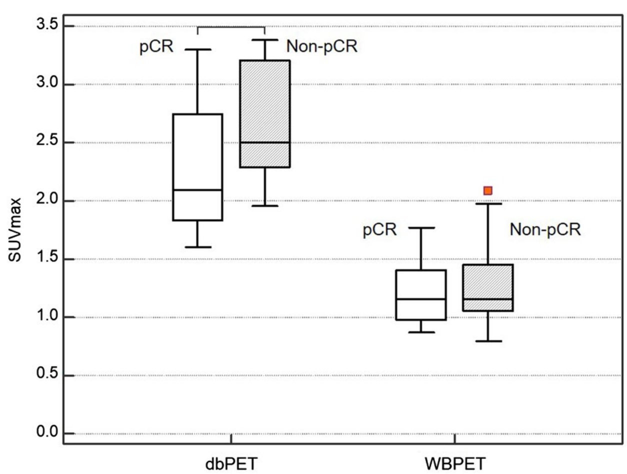

Fig. 1 Boxplots comparing SUV_{max} between non-pCR and pCR tumors in WBPET and dbPET scans. On dbPET, SUV_{max} was significantly higher in non-pCR than in pCR tumors (3.90 ± 3.15 vs 2.28 ± 0.60, $P = 0.030$). On WBPET, there was no significant difference in SUV_{max} between non-pCR than in pCR tumors (1.60 ± 0.92 vs 1.22 ± 0.30, $P = 0.30$)

Discussion

NAC has become a standard therapy for locally advanced breast cancer. However, it has previously been reported that WBPET does not provide an accurate assessment of residual tumor after primary chemotherapy for breast cancer, with sensitivity for the detection of residual tumor in the range 32.9–57.5% [16]. In our study, the sensitivity of 26.3% for the detection of residual tumor in the quantitative image analysis was comparable with the lower end of the range in the previous report.

The detectability of primary breast cancer can be significantly improved by adding dbPET to WBPET, especially for tumors smaller than 1 cm [8, 17–19]. In the present study, 21 out of 24 residual tumors (88%) were less than 1 cm in size. Because tumors contract after NAC, most residual tumors demonstrated no significant FDG uptake on WBPET even when there was still a histopathologically viable tumor. This was because of the limited spatial resolution of WBPET. On dbPET, which has better spatial resolution, we were able to detect more residual tumors, including those less than 1 cm in size. Indeed, only one of the 21 residual tumors could be detected on WBPET, compared with nine on dbPET, resulting in a significant improvement in sensitivity for the detection of residual tumor.

On dbPET, the SUV_{max} was significantly higher in non-pCR tumors than in pCR tumors. This meant that using dbPET significantly improved the sensitivity for the detection of residual tumor in the quantitative image analysis as well. However, even with dbPET, we detected residual tumors in only 50% of cases determined by the histopathological assessment. All the residual tumors over 7 mm were detected on dbPET, but some of the residual tumors sized 0.5–6 mm could not be detected, even with dbPET. Smaller lesions, especially scattered lesions, also proved difficult to detect on dbPET.

In this study, all the invasive lesions histopathologically disappeared, with only intraductal components remaining after NAC in five cases. One of these showed significant FDG uptake on dbPET, but this was not detected on WBPET. According to the histopathological assessment, the intraductal component formed a concentrated 4-mm mass. Even when there was only an intraductal component, we sometimes detected it as residual disease if the lesion formed a concentrated mass. Thus, the specificity of dbPET for the detection of a non-pCR tumor was lower than that of WBPET.

Our study had two limitations. First, we used only the ring-type dbPET. This has a relatively large blind area adjacent to the pectoral muscle. Asian countries have a greater number of patients with small breasts than is the case in Western countries. In such patients, some residual tumor was present but out of the imaging range. This limitation may lead to the misdiagnosis of tumor remnants or an incorrect evaluation of their extent. Second, our sample size was relatively small. Only 27 cases were included in the study population and there were only eight pCR tumors. The influence of selection bias may be great. Thus, further clinical studies are needed to investigate the utility of dbPET.

In conclusion, dbPET was superior to WBPET for the detection of residual tumor after NAC.

Table 4 Qualitative diagnostic performance for the detection of non-pCR tumor between WBPET and dbPET

	WBPET	DbPET	*P* value
Confidence rating			
pCR	1.0 ± 0.0 (1.0)	1.8 ± 1.4 (1.0–5.0)	0.10
Non-pCR	1.5 ± 1.3 (1.0–5.0)	3.1 ± 1.9 (1.0–5.0)	0.007*
P value	0.55	0.20	NA
Diagnostic performance			
Sensitivity	21.1% (4/19)	57.9% (11/19)	0.016*
Specificity	100.0% (8/8)	87.5% (7/8)	1.00
Positive predictive value	100.0% (4/4)	91.7%(11/12)	1.00
Negative predictive value	31.8% (7/22)	46.7% (7/15)	0.49
AUC (95% CI)	0.61 (0.40–0.79)	0.67 (0.46–0.84)	0.65

WBPET whole-body positron emission tomography, *dbPET* dedicated breast positron emission tomography, *pCR* pathological complete response, *AUC* area under the ROC curve, *CI* confidence interval, *NA* not applicable

*$P < 0.05$, significant difference

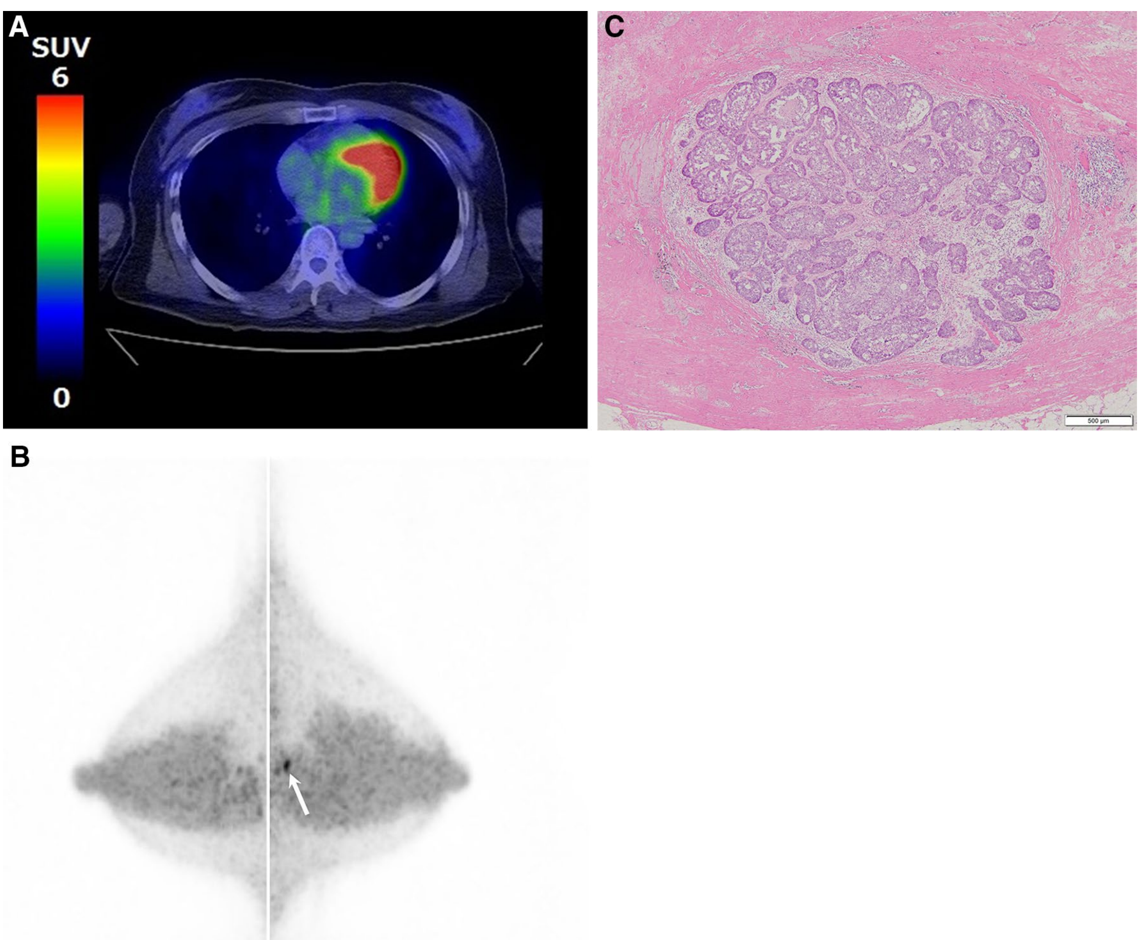

Fig. 2 A 44-year-old woman with left breast cancer. **a** Axial fusion WBPET image, showing no significant focal FDG uptake in the left breast (SUV_{max} of 1.61 in right breast and that of 1.72 in left breast). **b** Maximum-intensity projection dbPET image, showing a small amount of FDG uptake in the left breast. **c** Low-power microscopic view with hematoxylin and eosin staining, showing concentrated residual tumor cells 3 mm in diameter

Compliance with ethical standards

Conflict of interest The authors declare that they have no conflict of interest.

Ethical approval All procedures performed in studies were in accordance with the ethical standards of the institutional and/or national research committee and with the 1964 Helsinki Declaration and its later amendments or comparable ethical standards.

Informed consent Informed consent was obtained from all individual participants included in the study.

References

1. Groheux D, Espie M, Giacchetti S, Hindie E. Performance of FDG PET/CT in the clinical management of breast cancer. Radiology. 2013;266(2):388–405.
2. Bos R, van Der Hoeven JJ, van Der Wall E, van Der Groep P, van Diest PJ, Comans EF, et al. Biologic correlates of (18)fluorodeoxyglucose uptake in human breast cancer measured by positron emission tomography. J Clin Oncol. 2002;20(2):379–87.
3. Brown RS, Wahl RL. Overexpression of glut-1 glucose transporter in human breast cancer. An immunohistochemical study. Cancer. 1993;72(10):2979–85.
4. Kumar R, Chauhan A, Zhuang H, Chandra P, Schnall M, Alavi A. Clinicopathologic factors associated with false negative FDG-PET in primary breast cancer. Breast Cancer Res Treat. 2006;98(3):267–74.
5. Avril N, Rose CA, Schelling M, Dose J, Kuhn W, Bense S, et al. Breast imaging with positron emission tomography and fluorine-18 fluorodeoxyglucose: use and limitations. J Clin Oncol. 2000;18(20):3495–502.
6. Thompson CJ, Murthy K, Weinberg IN, Mako F. Feasibility study for positron emission mammography. Med Phys. 1994;21(4):529–38.
7. Garcia Hernandez T, Vicedo Gonzalez A, Ferrer Rebolleda J, Sanchez Jurado R, Rosello Ferrando J, Brualla Gonzalez L, et al. Performance evaluation of a high resolution dedicated breast PET scanner. Med Phys. 2016;43(5):2261.
8. Nishimatsu K, Nakamoto Y, Miyake KK, Ishimori T, Kanao S, Toi M, et al. Higher breast cancer conspicuity on dbPET compared to WB-PET/CT. Eur J Radiol. 2017;90:138–45.
9. van der Hage JA, van de Velde CJ, Julien JP, Tubiana-Hulin M, Vandervelden C, Duchateau L. Preoperative chemotherapy in primary operable breast cancer: results from the European Organization for Research and Treatment of Cancer trial 10902. J Clin Oncol. 2001;19(22):4224–37.
10. Choi M, Park YH, Ahn JS, Im YH, Nam SJ, Cho SY, et al. Assessment of pathologic response and long-term outcome in locally advanced breast cancers after neoadjuvant chemotherapy: comparison of pathologic classification systems. Breast Cancer Res Treat. 2016;160(3):475–89.
11. Cortazar P, Zhang L, Untch M, Mehta K, Costantino JP, Wolmark N, et al. Pathological complete response and long-term clinical benefit in breast cancer: the CTNeoBC pooled analysis. Lancet (Lond Engl). 2014;384(9938):164–72.
12. Mieog JS, van der Hage JA, van de Velde CJ. Preoperative chemotherapy for women with operable breast cancer. Cochrane Database Syst Rev. 2007;(2):Cd005002.
13. Yeh E, Slanetz P, Kopans DB, Rafferty E, Georgian-Smith D, Moy L, et al. Prospective comparison of mammography, sonography, and MRI in patients undergoing neoadjuvant chemotherapy for palpable breast cancer. AJR Am J Roentgenol. 2005;184(3):868–77.
14. Chen JH, Bahri S, Mehta RS, Kuzucan A, Yu HJ, Carpenter PM, et al. Breast cancer: evaluation of response to neoadjuvant chemotherapy with 3.0-T MR imaging. Radiology. 2011;261(3):735–43.
15. Kurosumi M, Akashi-Tanaka S, Akiyama F, Komoike Y, Mukai H, Nakamura S, et al. Histopathological criteria for assessment of therapeutic response in breast cancer (2007 version). Breast Cancer (Tokyo Jpn). 2008;15(1):5–7.
16. Dose-Schwarz J, Tiling R, Avril-Sassen S, Mahner S, Lebeau A, Weber C, et al. Assessment of residual tumour by FDG-PET: conventional imaging and clinical examination following primary chemotherapy of large and locally advanced breast cancer. Br J Cancer. 2010;102(1):35–41.
17. Eo JS, Chun IK, Paeng JC, Kang KW, Lee SM, Han W, et al. Imaging sensitivity of dedicated positron emission mammography in relation to tumor size. Breast (Edinb Scotl). 2012;21(1):66–71.
18. Kalinyak JE, Berg WA, Schilling K, Madsen KS, Narayanan D, Tartar M. Breast cancer detection using high-resolution breast PET compared to whole-body PET or PET/CT. Eur J Nucl Med Mol Imaging. 2014;41(2):260–75.
19. Yamamoto Y, Ozawa Y, Kubouchi K, Nakamura S, Nakajima Y, Inoue T. Comparative analysis of imaging sensitivity of positron emission mammography and whole-body PET in relation to tumor size. Clin Nucl Med. 2015;40(1):21–5.